# Supplementary information

## Deciphering the Chemical Bond of Trivalent Oxygen Atom in Oxygen Doped Graphene

Andoni Ugartemendia,[1,2] Irene Casademont-Reig,[3] Lili Zhao[4], Zuxian Zhang[4], Gernot Frenking,[2,4,5] Jesus M. Ugalde,[1,2] Aran Garcia-Lekue[2,6,*] and Elisa Jimenez-Izal[1,2,*]

[1] *Polimero eta Material Aurreratuak: Fisika, Kimika eta Teknologia Saila, Kimika Fakultatea, Euskal Herriko Unibertsitatea (UPV/EHU), M. de Lardizabal Pasealekua 3, Donostia, Euskadi, Spain*
[2] *Donostia International Physics Center (DIPC), M. de Lardizabal Pasealekua 3, Donostia, Euskadi, Spain*
[3] *Department of General Chemistry (ALGC), Vrije Universiteit Brussel (VUB), Pleinlaan 2, 1050 Brussels, Belgium*
[4] *Institute of Advanced Synthesis, School of Chemistry and Molecular Engineering, Jiangsu National Synergetic Innovation Center for Advanced Materials, Nanjing Tech University, Nanjing 211816, China*
[5] *Fachbereich Chemie, Philipps-Universität Marburg, Hans-Meerwein-Strasse, D-35043 Marburg, Germany*
[6] *IKERBASQUE, Basque Foundation for Science, Bilbao, Euskadi, Spain*

*E-mail: elisa.jimenez@ehu.es; wmbgalea@ehu.eus*

**Table of contents**.

## 1. Relaxed scan of graphitic oxygen

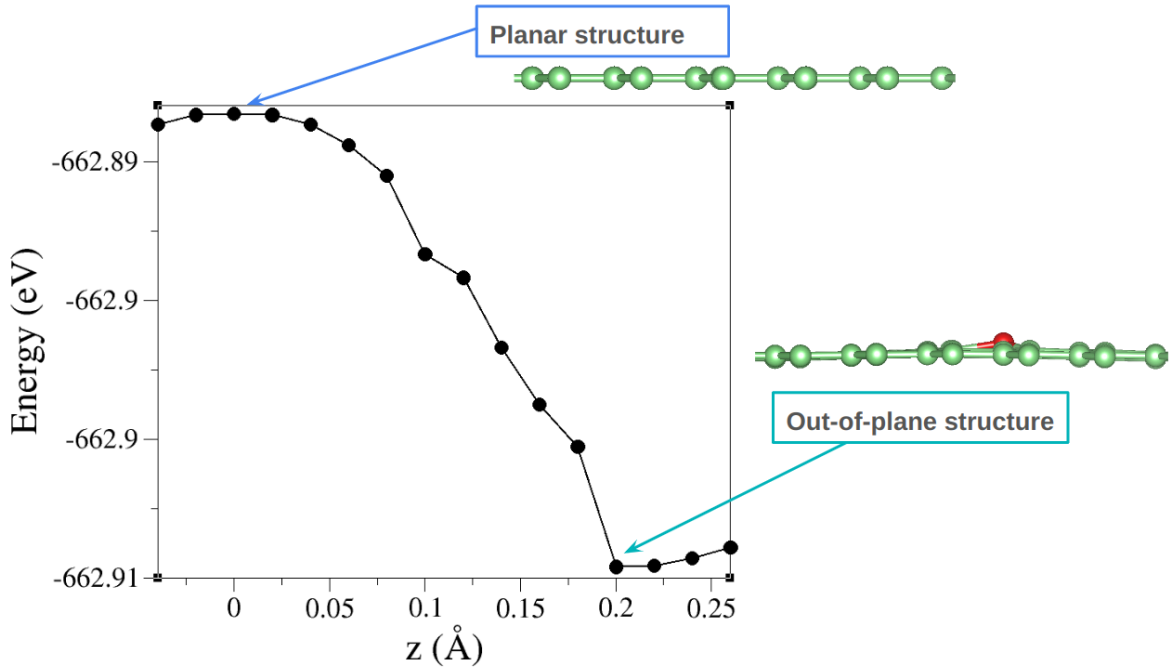


**Fig. S1.** Energy change of the grafitic oxygen system as a function of the O height (z in Å) with respect to the plane.

In Figure S1 it can be clearly seen that the out-of-plane structure, where oxygen is 0.2 Å out of plane, is a minimum in the potential energy surface, whereas the completely planar structure is not.

## 2. Charge density difference (CDD) between oxygen and graphene in periodic graphitic oxygen

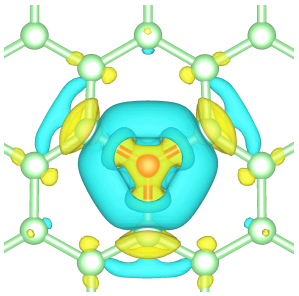

**Fig. S2.** Charge density difference (CDD) between oxygen and graphene in periodic graphitic oxygen. The yellow and cyan colors represent electron accumulation and depletion regions, respectively.

## 3. pCOHP plots

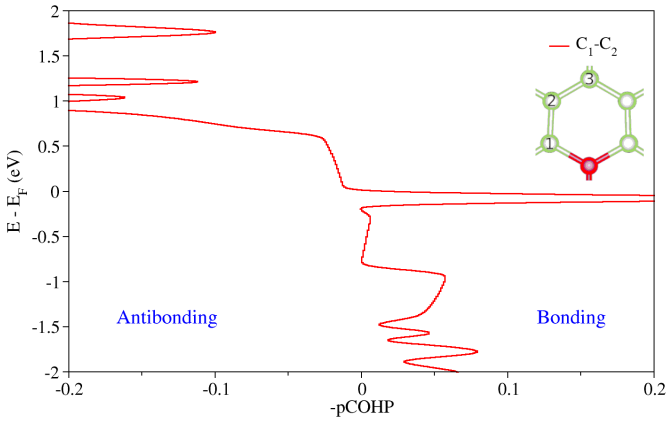


**Fig. S3.** pCOHP plot between $C_1$ $p_z$ and $C_2$ $p_z$ orbitals. Positive -pCOHP values correspond to bonding interactions, while negative -pCOHP to antibonding interactions, respectively. The energy is given with respect to the Fermi energy ($E_F$).

## 4. Delocalization indexes of fragment molecules

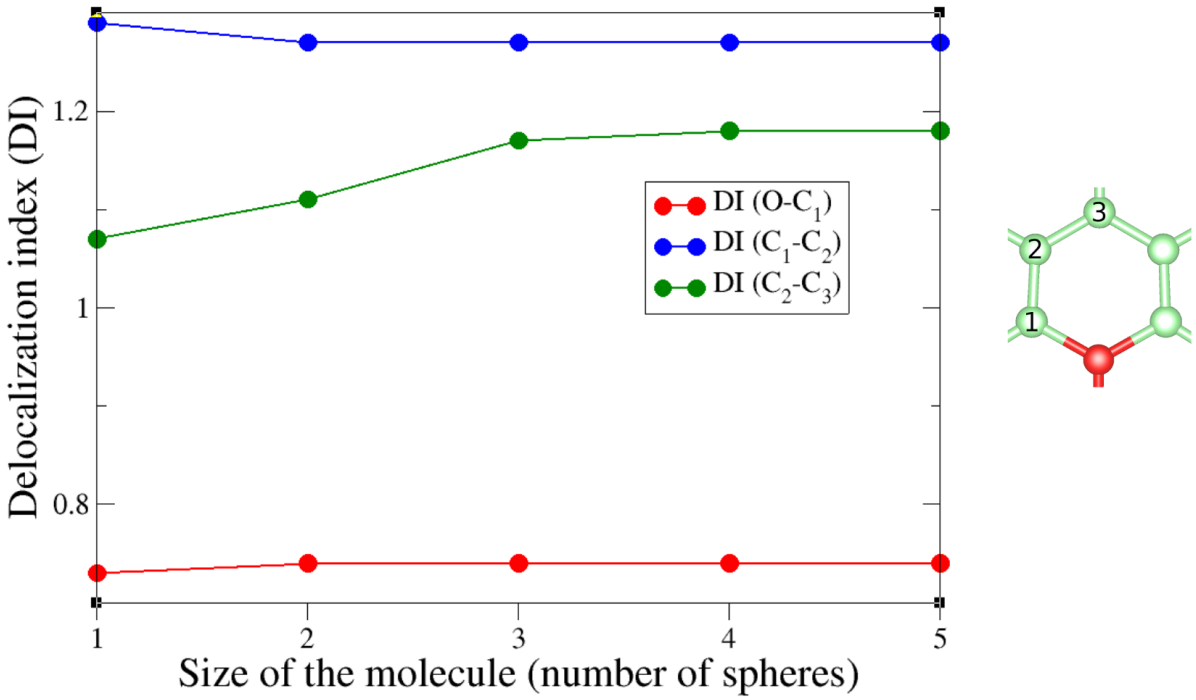


**Fig. S4**. Convergence of Delocalization Indexes with the size of the model molecules (1 sphere stands for $[OC_{12}H_9]^{7+}$, 2 spheres stands for $[OC_{36}H_{15}]^{13+}$, 3 spheres stands for $[OC_{72}H_{21}]^{19+}$, 4 spheres stands for $[OC_{120}H_{27}]^{25+}$, and 5 spheres stands for $[OC_{180}H_{33}]^{31+}$.

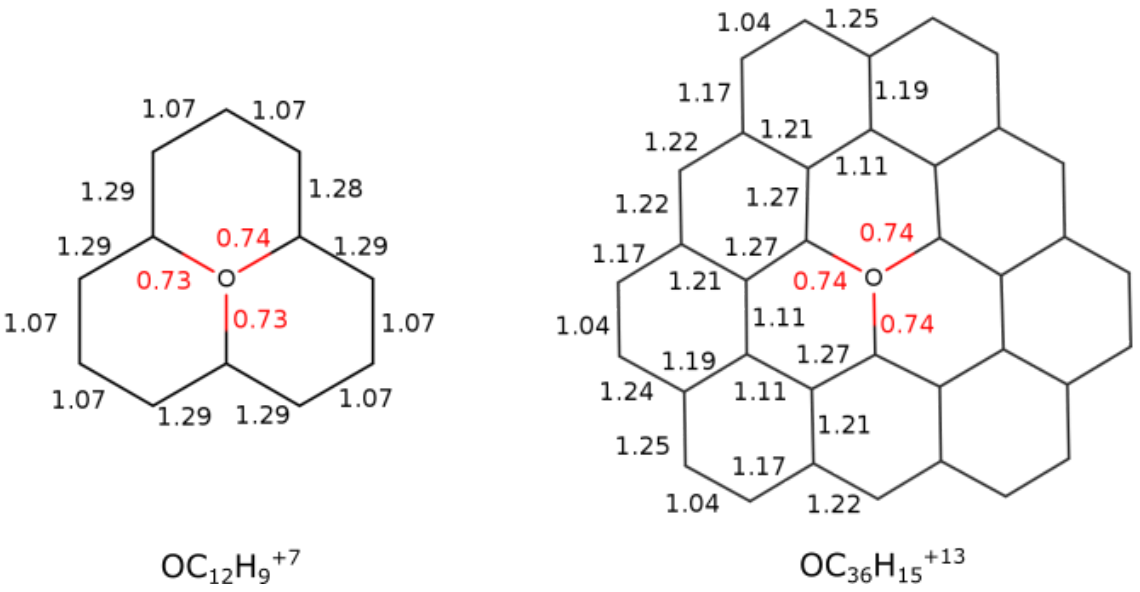


**Fig. S5**. Delocalization indexes of $[OC_{12}H_9]^{7+}$ and $[OC_{36}H_{15}]^{13+}$.

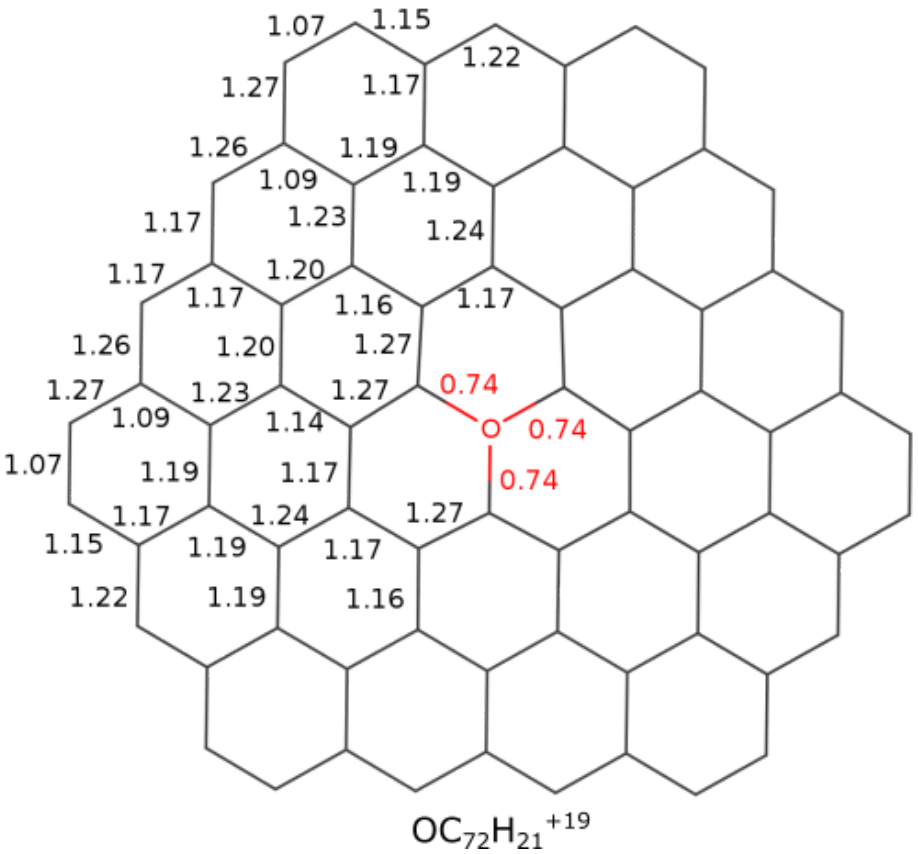


**Fig. S6**. Delocalization indexes of $[OC_{72}H_{21}]^{19+}$.

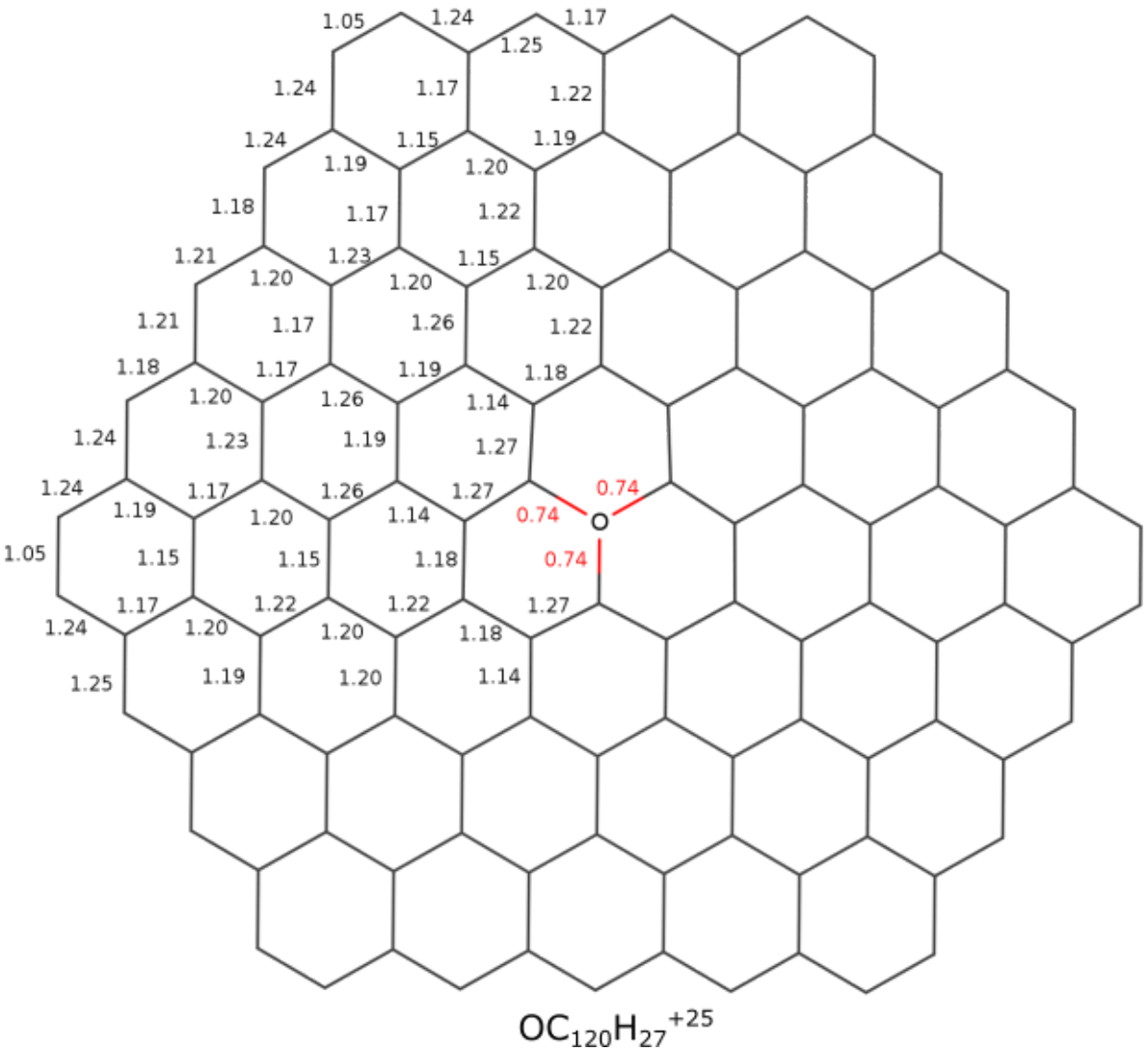


**Fig. S7**. Delocalization indexes of $[OC_{120}H_{27}]^{25+}$.

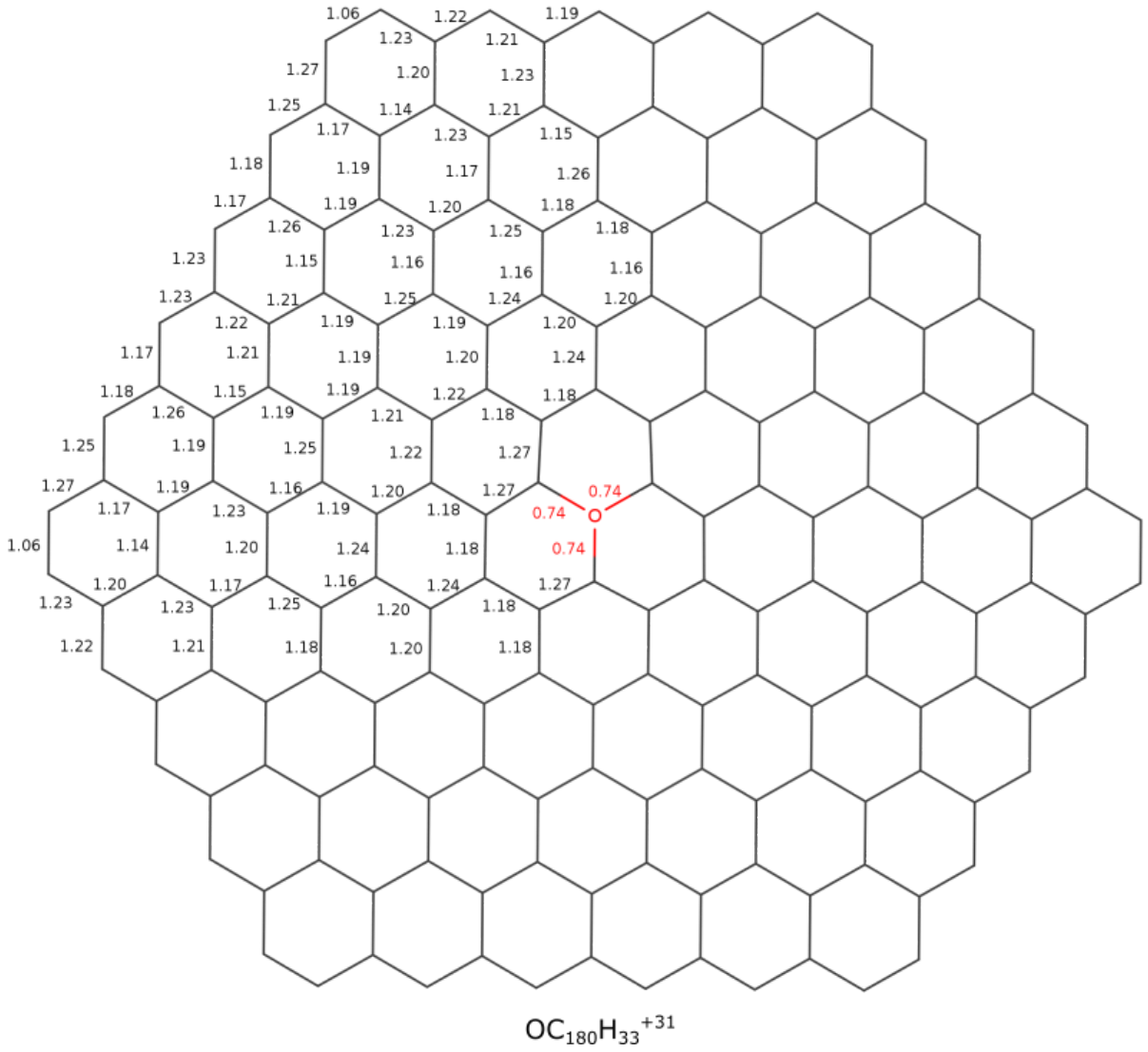


**Fig. S8**. Delocalization indexes of $[OC_{180}H_{33}]^{31+}$.

**5. ELF plots**

We computed the Electron Localization Function (ELF) on both the 2D and the model molecule, $(OC_{72}H_{21})^{19+}$. In Figure S8, two ELF slices are plotted. On the one hand ELF is plotted in the best plane that contains the O atom and nearby C atoms, since the system is not completely planar. Such a plane is just slightly tilted with respect to the molecular plane. And the second ELF slice is plotted 0.5 Å above that plane. As expected, the same picture is obtained for the 2D system and for the molecule. In both of them high electron localization regions can be identified in the middle between adjacent C-C bonds, suggesting non-polar σ bonds. Between C-O, high localization regions are identified although they are closer to oxygen, due to the electronegativity difference, suggesting polarized σ C-O bonds. Comparing both planes displaying the ELF, it could be easily observed that the extended surface and the molecular model behave in the same way, validating the combination of periodic calculations with a fragmental approach used in our work.

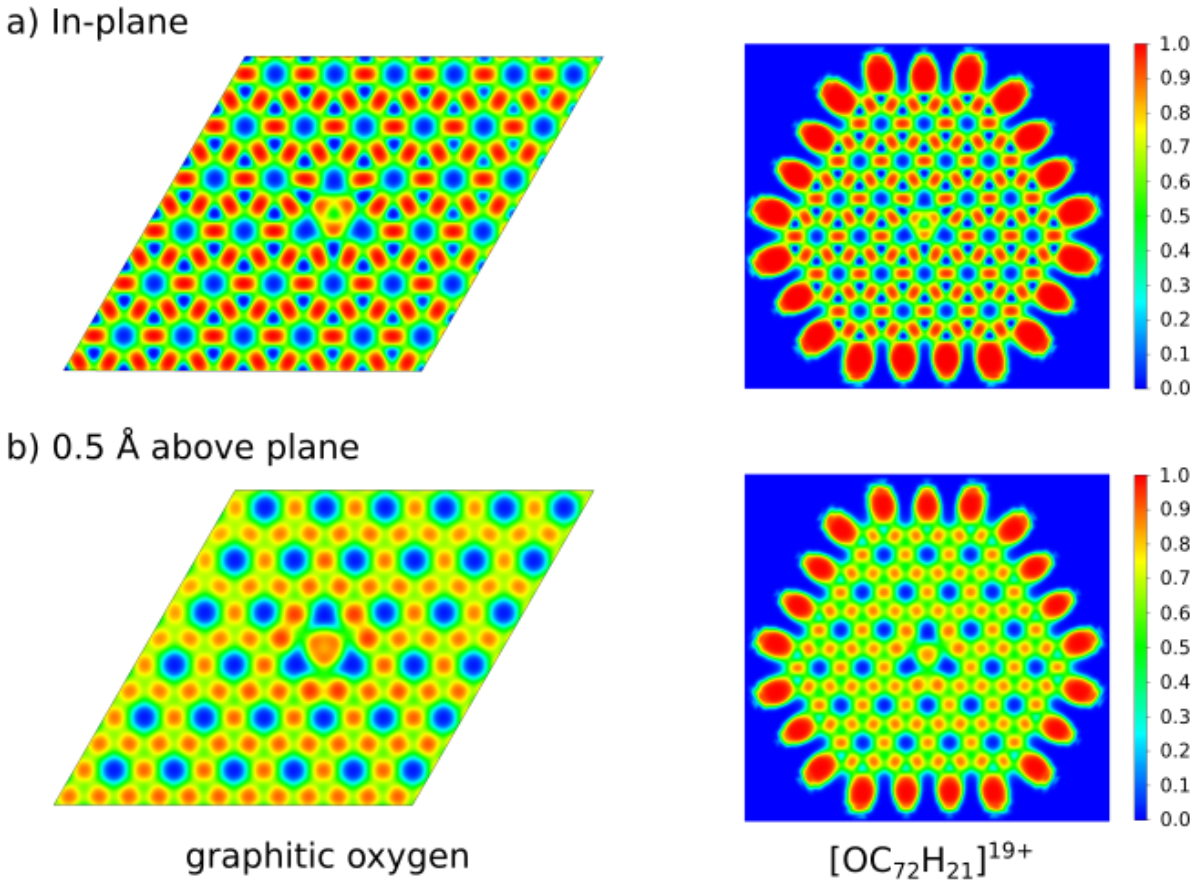


**Figure S9.** Electron localization function (ELF) profile of graphitic oxygen on the left, and the model molecule $(OC_{72}H_{21})^{19+}$ on the right, a) in the molecular plane, and b) 0.5 Å above the plane.

## 6. EDA-NOCV of fragment molecules

### EDA-NOCV analysis of $[C_{72}H_{21}]^{19+}$

**Fig. S10**. Plot of deformation densities Δρ of the pairwise orbital interactions between the two fragments of O (T) and $[C_{72}H_{21}]^{19+}$(T) in $[OC_{72}H_{21}]^{19+}$ (**Cs**, S) together with the associated interaction energies $\Delta E_{orb}$ (in kcal/mol). The eigenvalues v are a measure for the relative amount of charge transfer. The direction of the charge flow is from red to blue.

---

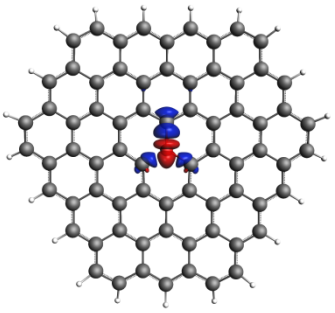

$\Delta E_{orb(2\alpha)}$ = -55.8 kcal/mol
$v_{2\alpha}$ = ± 0.418

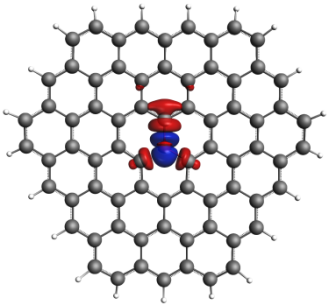

$\Delta E_{orb(2\beta)}$ = -148.9 kcal/mol
$v_{2\beta}$ = ± 0.714

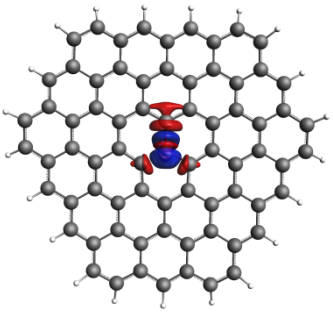

c
$\Delta E_{orb1} = \Delta E_{orb(2\alpha)} + \Delta E_{orb(2\beta)}$ = -204.7 kcal/mol

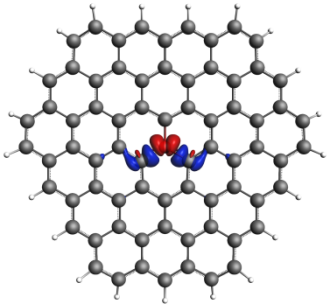

$\Delta E_{orb(3\alpha)}$ = -55.5 kcal/mol
$v_{3\alpha}$ = ± 0.418

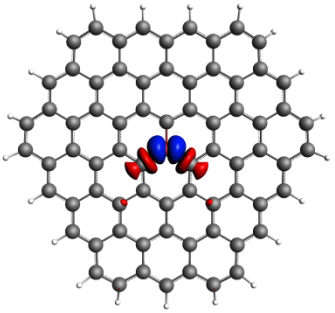

$\Delta E_{orb(3\beta)}$ = -142.0 kcal/mol
$v_{3\beta}$= ± 0.687

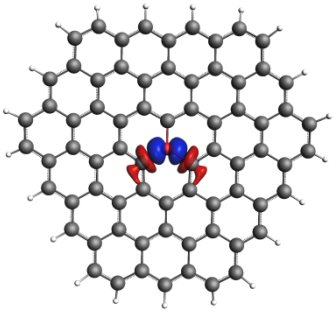

$\Delta E_{orb2} = \Delta E_{orb(3\alpha)} + \Delta E_{orb(3\beta)} = -197.5$ kcal/mol

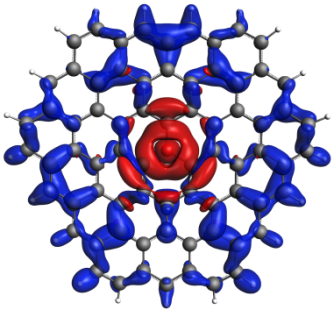

$\Delta E_{orb(1\alpha)} = -67.6$ kcal/mol

$v_{1\alpha} = \pm 0.732$

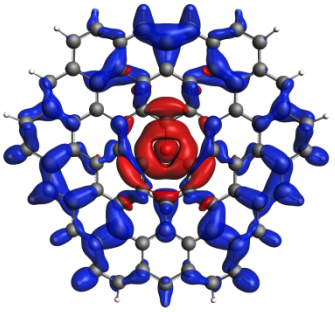

$\Delta E_{orb(1\beta)} = -66.1$ kcal/mol

$v_{1\beta} = \pm 0.732$

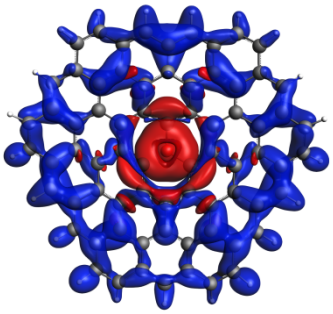

$\Delta E_{orb3} = \Delta E_{orb(1\alpha)} + \Delta E_{orb(1\beta)} = -133.7$ kcal/mol

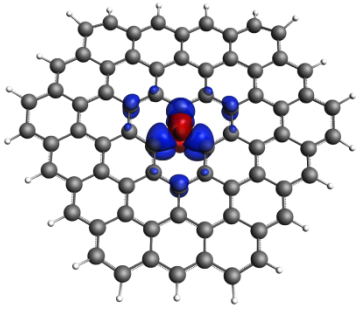

$\Delta E_{orb(6\alpha)} = -12.6$ kcal/mol

$v_{6\alpha} = \pm 0.226$

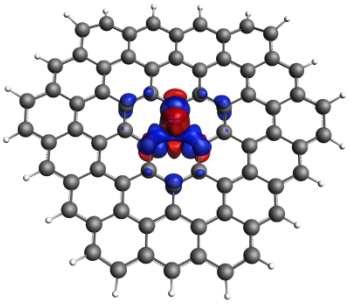

$\Delta E_{orb(6\beta)} = -15.9$ kcal/mol

$v_{6\beta} = \pm 0.226$

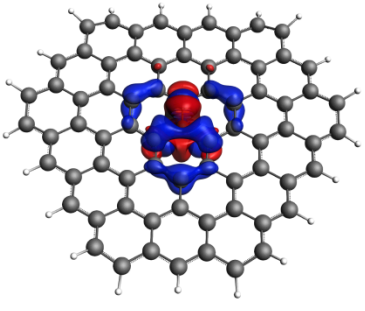

$\Delta E_{orb4} = \Delta E_{orb(6\alpha)} + \Delta E_{orb(6\beta)} = -28.5$ kcal/mol

**Fig. S11**. Plot of deformation densities Δρ of the pairwise orbital interactions and the associated interaction energies ($\Delta E_{orb}$) between fragments, as well as the shape of the most important interacting MOs of the two fragments **O (T)** and $[C_{72}H_{21}]^{19+}$**(T)** in $[OC_{72}H_{21}]^{19+}$ (D3h). The direction of the charge flow is red to blue.

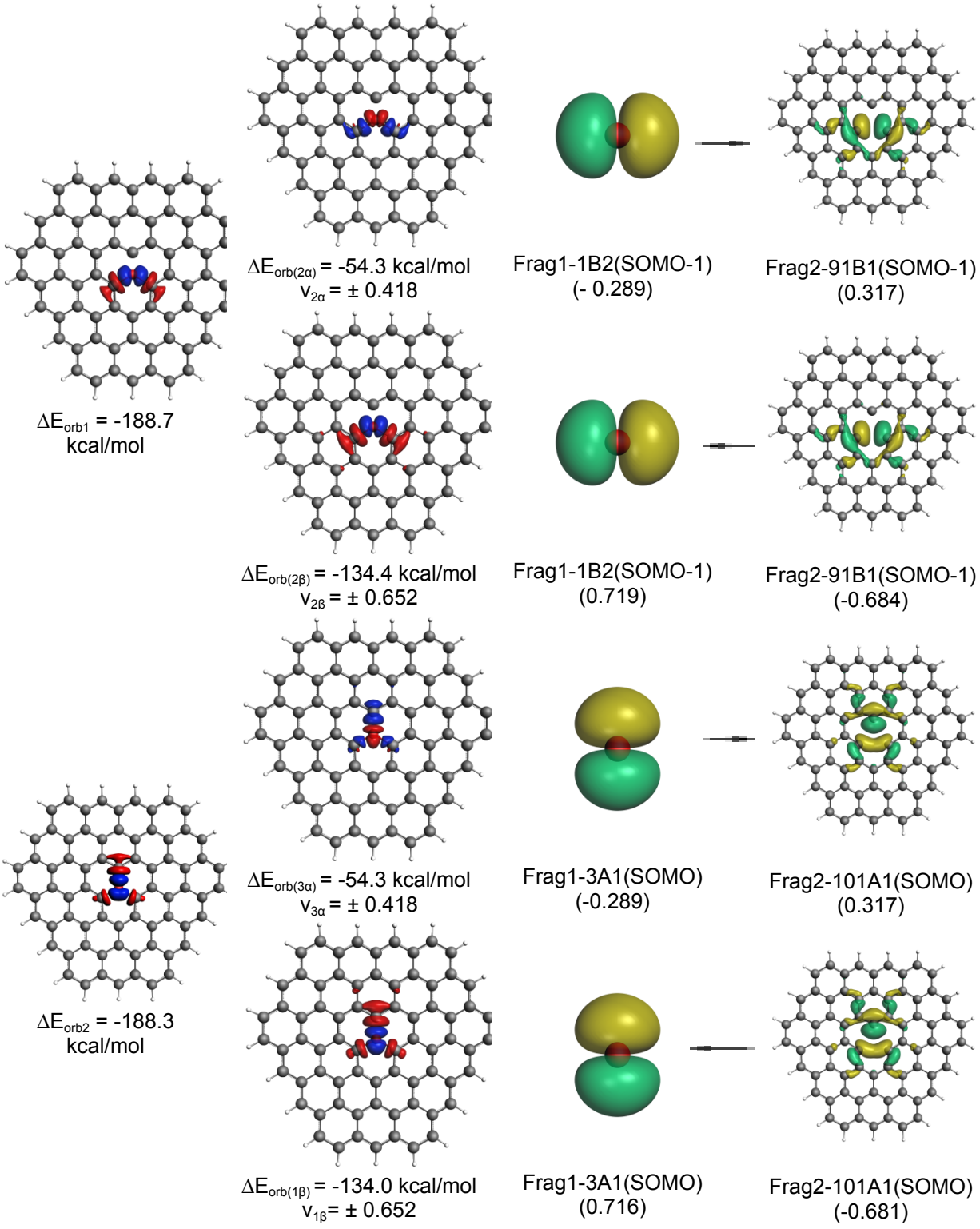

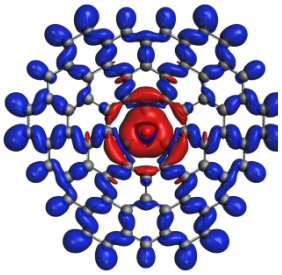

$\Delta E_{orb3}$= -109.8 kcal/mol

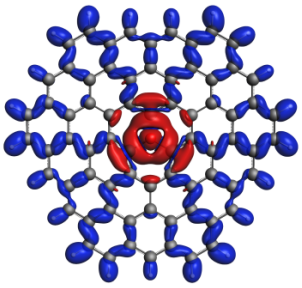

$\Delta E_{orb(1\alpha)}$ = -55.3 kcal/mol
$v_{1\alpha}$ = ± 0.650

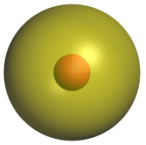

Frag1-2A1(HOMO-1)
(-0.131)

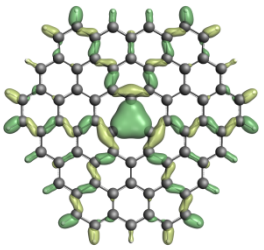

Frag2-100A1(LUMO)
(0.556)

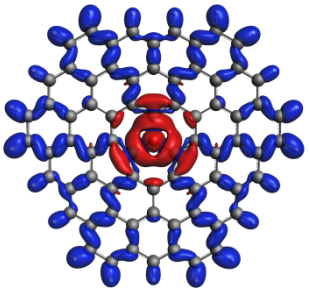

$\Delta E_{orb(3\beta)}$ = -54.5 kcal/mol
$v_{3\beta}$ = ± 0.650

Frag1-2A1(HOMO-1)
(-0.130)

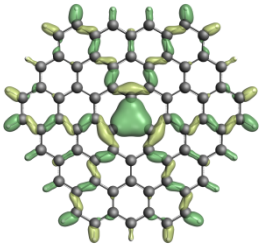

Frag2-100A1(LUMO)
(0.563)

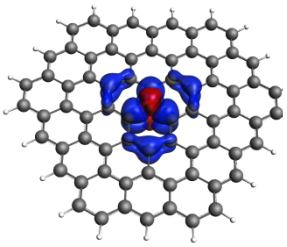

$\Delta E_{orb4}$= -27.2 kcal/mol

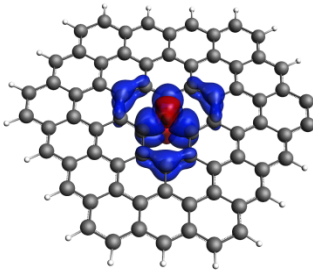

$\Delta E_{orb(6\alpha)}$ = -12.6 kcal/mol
$v_{6\alpha}$ = ± 0.227

Frag1-1B1(HOMO)
(-0.091)

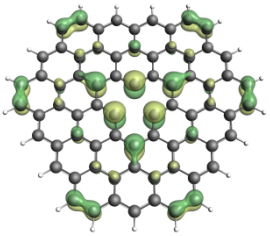

Frag2-18B1(LUMO-6)
(0.046)

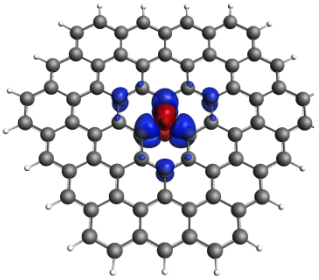

$\Delta E_{orb(6\beta)}$ = -14.6 kcal/mol
$v_{6\beta}$ = ± 0.227

Frag1-1B1(HOMO)
(-0.091)

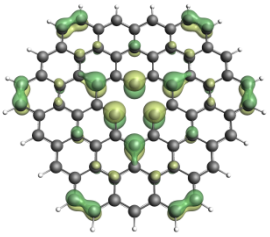

Frag2-18B1(LUMO-6)
(0.046)

**Table S1**. EDA-NOCV results of $[OC_{72}H_{21}]^{19+}$ (**Cs**, S) at the BP86-D3(BJ)/def2-TZ2P level of theory. Fragments are given in singlet (S), triplet (T) electronic states. Energy values are given in kcal/mol.

| Fragments | O(T) + $[C_{72}H_{21}]^{19+}$(T) | O(S) + $[C_{72}H_{21}]^{19+}$(S) |
|---|---|---|
| $\Delta E_{int}$ | -324.8 | -954.9 |
| $\Delta E_{Pauli}$ | 542.3 | 287.6 |
| $\Delta E_{elstat}$[a] | -257.2(29.7%) | -349.8(28.2%) |
| $\Delta E_{disp}$[a] | -2.8(0.3%) | -2.8(0.2%) |
| $\Delta E_{orb}$[a] | -607.1(70.0%) | -889.9(71.6%) |
| $\Delta E_{orb1}$[b] | -204.7(33.7%) | |
| $\Delta E_{orb2}$[b] | -197.5(32.5%) | |
| $\Delta E_{orb3}$[b] | -133.7(22.0%) | |
| $\Delta E_{orb4}$[b] | -28.5(4.7%) | |
| $\Delta E_{orb(rest)}$[b] | -42.7(7.1%) | |

[a]The values in parentheses give the percentage contribution to the total attractive interactions $\Delta E_{elstat} + \Delta E_{orb} + \Delta E_{disp.}$
[b]The values in parentheses give the percentage contribution to the total orbital interactions $\Delta E_{orb}$.

**Table S2**. EDA-NOCV results of $[OC_{72}H_{21}]^{19+}$ (**C3v**, S) at the BP86-D3(BJ)/def2-TZ2P level of theory. Fragments are given in singlet (S), triplet (T) electronic states. Energy values are given in kcal/mol.

| Fragments | O(T) + $[C_{72}H_{21}]^{19+}$(T) | O(S) + $[C_{72}H_{21}]^{19+}$(S) |
|---|---|---|
| $\Delta E_{int}$ | -363.2 | -955.0 |
| $\Delta E_{Pauli}$ | 450.7 | 286.4 |
| $\Delta E_{elstat}$[a] | -199.1(24.5%) | -349.7(28.2%) |
| $\Delta E_{disp}$[a] | -2.8(0.3%) | -2.8(0.2%) |
| $\Delta E_{orb}$[a] | -611.9(75.2%) | -889.0(71.6%) |
| $\Delta E_{orb1}$[b] | -216.6(35.4%) | |
| $\Delta E_{orb2}$[b] | -216.6(35.4%) | |
| $\Delta E_{orb3}$[b] | -115.4(18.9%) | |
| $\Delta E_{orb4}$[b] | -22.9(3.7%) | |
| $\Delta E_{orb(rest)}$[b] | -40.4(6.6%) | |

[a]The values in parentheses give the percentage contribution to the total attractive interactions $\Delta E_{elstat} + \Delta E_{orb} + \Delta E_{disp.}$
[b]The values in parentheses give the percentage contribution to the total orbital interactions $\Delta E_{orb}$.

## EDA-NOCV analysis of $[OC_{36}H_{15}]^{13+}$ and $OC_{36}H_{15}$

**Table S3**. EDA-NOCV results of **$[OC_{36}H_{15}]^{13+}$** (**D3h**, S) at the BP86-D3(BJ)/def2-TZ2P level of theory. Fragments are given in singlet (S), doublet (D) or triplet (T) electronic states. Energy values are given in kcal/mol.

| **Fragments** | **O(T) + $[C_{36}H_{15}]^{13+}$(T)** | **O(S) + $[C_{36}H_{15}]^{13+}$(S)** | **$O^{-1}$(D) + $[C_{36}H_{15}]^{14+}$(D)** |
|---|---|---|---|
| $\Delta E_{int}$ | -312.8 | -949.4 | -1653.6 |
| $\Delta E_{Pauli}$ | 414.6 | 286.6 | 599.8 |
| $\Delta E_{elstat}$[a] | -201.5(27.7%) | -337.0(27.3%) | -1478.0(63.8%) |
| $\Delta E_{disp}$[a] | -2.8(0.4%) | -2.8(0.2%) | -2.8(0.1%) |
| $\Delta E_{orb}$[a] | -523.2(71.9%) | -896.2(72.5%) | -772.6(36.1%) |
| $\Delta E_{orb1}$[b] | -186.2(35.6%) | | |
| $\Delta E_{orb2}$[b] | -186.1(35.6%) | | |
| $\Delta E_{orb3}$[b] | -86.4(16.5%) | | |
| $\Delta E_{orb4}$[b] | -25.9(4.9%) | | |
| $\Delta E_{orb(rest)}$[b] | -38.6(7.4%) | | |

[a]The values in parentheses give the percentage contribution to the total attractive interactions $\Delta E_{elstat} + \Delta E_{orb} + \Delta E_{disp.}$

[b]The values in parentheses give the percentage contribution to the total orbital interactions $\Delta E_{orb}$.

**Fig. S12**. Plot of deformation densities Δρ of the pairwise orbital interactions and the associated interaction energies ($\Delta E_{orb}$) between fragments, as well as the shape of the most important interacting MOs of the two fragments O (T) and $[C_{36}H_{15}]^{13+}$(T) in **$[OC_{36}H_{15}]^{13+}$** (**D3h**, S), The direction of the charge flow is red to blue.

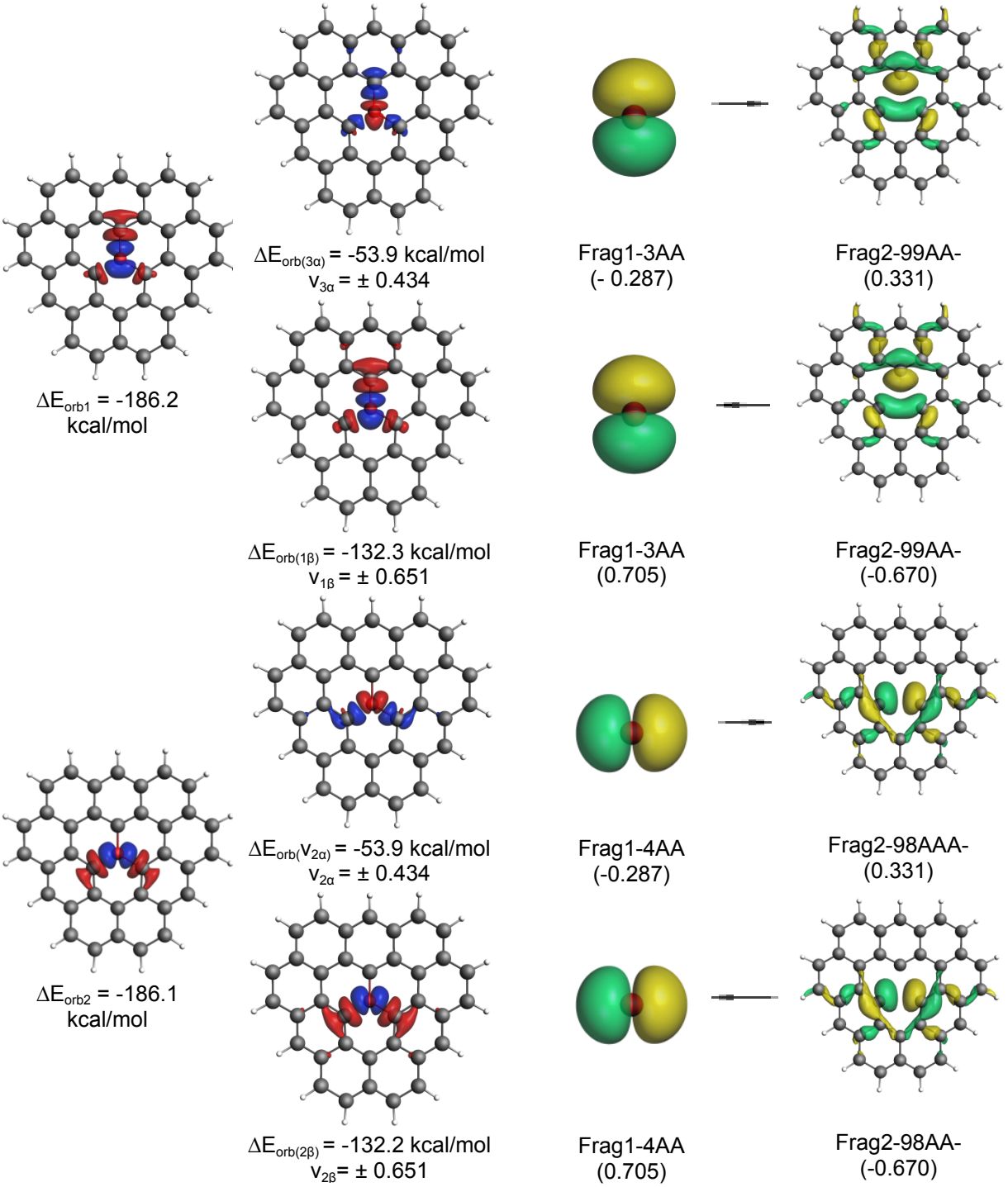

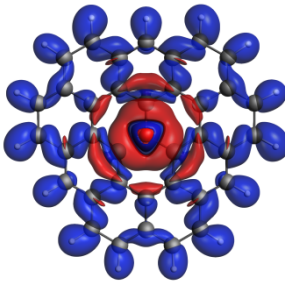

$\Delta E_{orb3}$= -86.4 kcal/mol

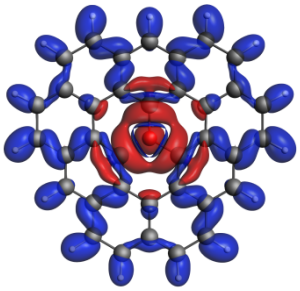

$\Delta E_{orb(1\alpha)}$ = -43.1 kcal/mol
$v_{1\alpha}$ = ± 0.536

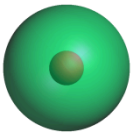

Frag1-2AA
(-0.127)

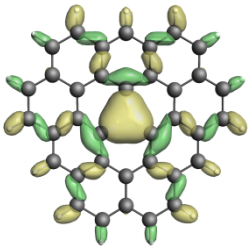

Frag2-97AA
(0.429)

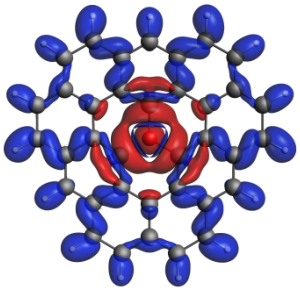

$\Delta E_{orb(3\beta)}$ = -43.3 kcal/mol
$v_{3\beta}$ = ± 0.536

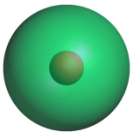

Frag1-2AA
(-0.127)

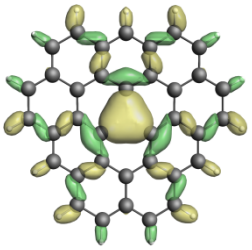

Frag2-97AA
(0.429)

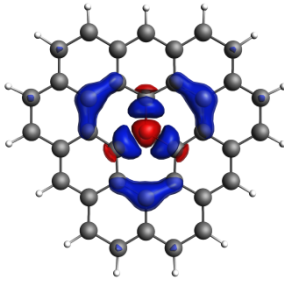

$\Delta E_{orb4}$ = -25.9 kcal/mol

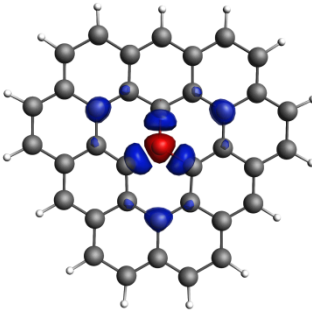

$\Delta E_{orb(6\alpha)}$ = -12.0 kcal/mol
$v_{6\alpha}$ = ± 0.235

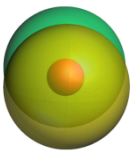

Frag1-1AAA
(-0.094)

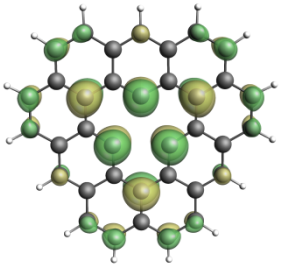

Frag2-16AAA
(0.074)

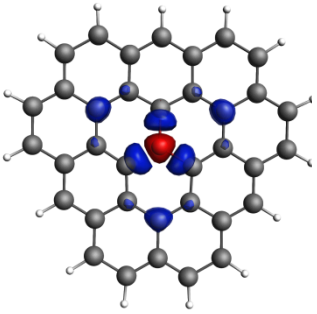

$\Delta E_{orb(6\beta)}$ = -13.9 kcal/mol
$v_{6\beta}$ = ± 0.235

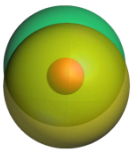

Frag1-1AAA
(-0.094)

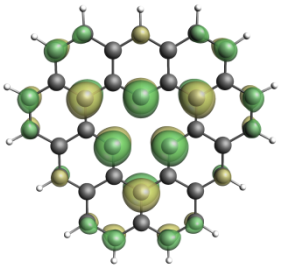

Frag2-16AAA
(0.074)

**Table S4**. EDA-NOCV results of **[$OC_{36}H_{15}$]** (D3h, D) at the BP86-D3(BJ)/def2-TZ2P level of theory. Fragments are given in singlet (S), doublet (D), triplet (T) or quartet(Q) electronic states. Energy values are given in kcal/mol.

| **Fragments** | **O(T) + $[C_{36}H_{15}]$(Q)** | **O(S) + $[C_{36}H_{15}]$(D)** | **$O^{-1}$(D) + $[C_{36}H_{15}]^{+}$(S)** | **$O^{-2}$(S) + $[C_{36}H_{15}]^{2+}$(D)** |
|---|---|---|---|---|
| $\Delta E_{int}$ | -327.9 | -922.2 | -480.5 | -878.0 |
| $\Delta E_{Pauli}$ | 410.5 | 363.8 | 857.9 | 973.9 |
| $\Delta E_{elstat}$[a] | -197.1(27.7%) | -410.4(31.9%) | -639.3(47.8%) | -1022.7(55.2%) |
| $\Delta E_{disp}$[a] | -2.7(0.4%) | -2.7(0.2%) | -2.7(0.2%) | -2.7(0.2%) |
| $\Delta E_{orb}$[a] | -538.6(71.9%) | -872.9(67.9%) | -696.5(52.0%) | -826.5(44.6%) |
| $\Delta E_{orb1}$[b] | -204.2(37.9%) | | | |
| $\Delta E_{orb2}$[b] | -204.2(37.9%) | | | |
| $\Delta E_{orb3}$[b] | -77.5(14.4%) | | | |
| $\Delta E_{orb4}$[b] | -10.2(1.9%) | | | |
| $\Delta E_{orb(rest)}$[b] | -42.5(7.9%) | | | |

[a]The values in parentheses give the percentage contribution to the total attractive interactions $\Delta E_{elstat} + \Delta E_{orb} + \Delta E_{disp.}$

[b]The values in parentheses give the percentage contribution to the total orbital interactions $\Delta E_{orb}$.

**Figure S13**. Plot of deformation densities Δρ of the pairwise orbital interactions and the associated interaction energies ($\Delta E_{orb}$) between fragments, as well as the shape of the most important interacting MOs of the two fragments O (T) and [$C_{36}H_{15}$] (Q) in **[$OC_{36}H_{15}$]** (**D3h**, D), The direction of the charge flow is red to blue.

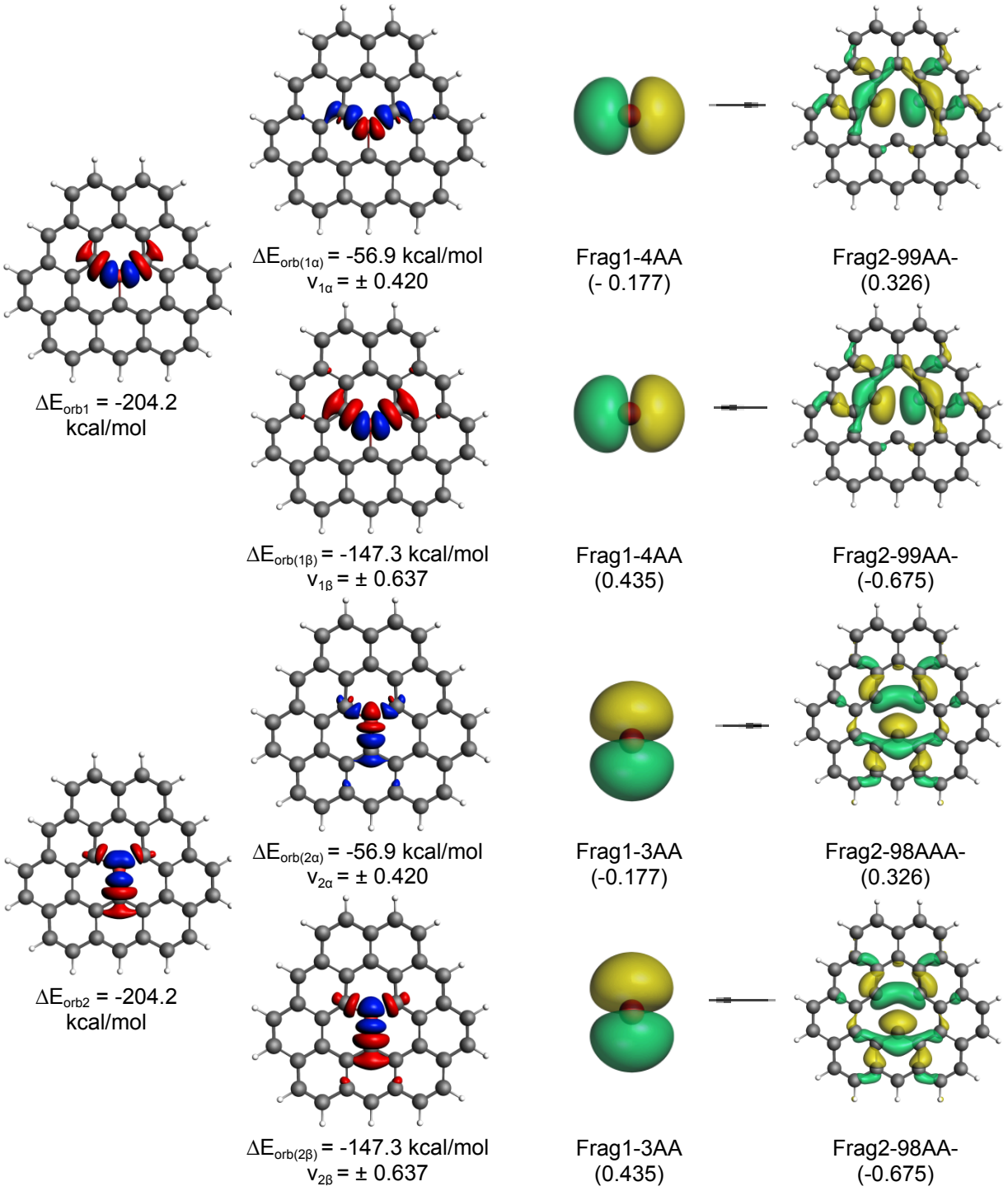

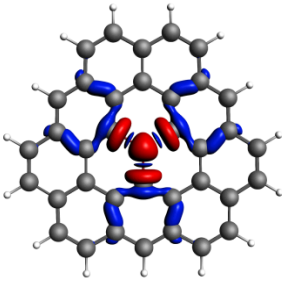

$\Delta E_{orb3}$ = -77.5 kcal/mol

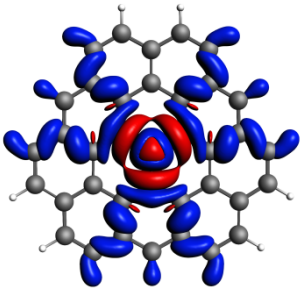

$\Delta E_{orb(3\alpha)}$ = -36.6 kcal/mol
$v_{3\alpha}$ = ± 0.371

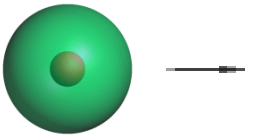

Frag1-2AA
(-0.148)

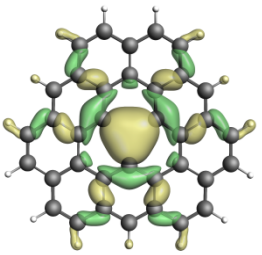

Frag2-97AA
(0.296)

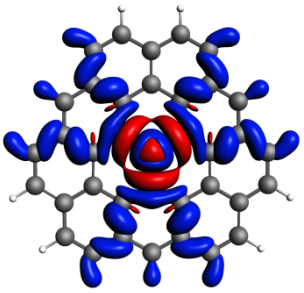

$\Delta E_{orb(3\beta)}$ = -40.9 kcal/mol
$v_{3\beta}$ = ± 0.374

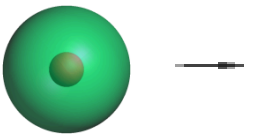

Frag1-2AA
(-0.149)

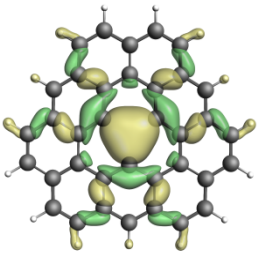

Frag2-97AA
(0.298)

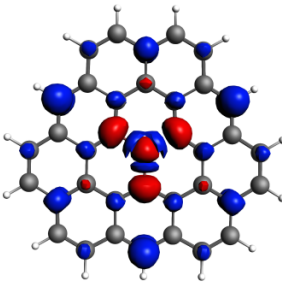

$\Delta E_{orb4}$ = -10.2 kcal/mol

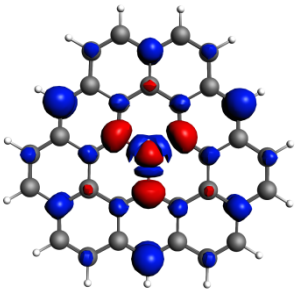

$\Delta E_{orb(4\beta)}$ = -10.2 kcal/mol
$v_{4\beta}$ = ± 0.252

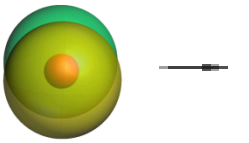

Frag1-1AAA
(-0.075)

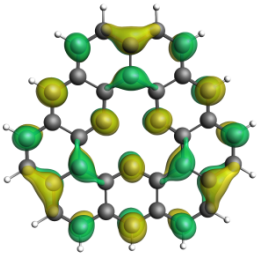

Frag2-19AAA
(0.072)